Ocean Science

Measuring rates of present-day relative sea-level rise in low-elevation coastal zones: a critical evaluation

Molly E. Keogh and Torbjörn E. Törnqvist

Department of Earth and Environmental Sciences, Tulane University, 6823 St. Charles Avenue,
New Orleans, Louisiana 70118-5698, USA

Correspondence: Molly E. Keogh (mkeogh@tulane.edu)

Abstract. Although tide gauges are the primary source of data used to calculate multi-decadal- to century-scale rates of relative sea-level change, we question the usefulness of tide-gauge data in rapidly subsiding low-elevation coastal zones (LECZs). Tide gauges measure relative sea-level rise (RSLR) with respect to the base of associated benchmarks. Focusing on coastal Louisiana, the largest LECZ in the United States, we find that these benchmarks ($n = 35$) are anchored an average of 21.5 m below the land surface. Because at least 60 % of subsidence occurs in the top 5 m of the sediment column in this area, tide gauges in coastal Louisiana do not capture the primary contributor to RSLR. Similarly, global navigation satellite system (GNSS) stations ($n = 10$) are anchored an average of > 14.3 m below the land surface and therefore also do not capture shallow subsidence. As a result, tide gauges and GNSS stations in coastal Louisiana, and likely in LECZs worldwide, systematically underestimate rates of RSLR as experienced at the land surface. We present an alternative approach that explicitly measures RSLR in LECZs with respect to the land surface and eliminates the need for tide-gauge data in this context. Shallow subsidence is measured by rod surface-elevation table–marker horizons (RSET-MHs) and added to measurements of deep subsidence from GNSS data, plus sea-level rise from satellite altimetry. We show that for an LECZ the size of coastal Louisiana (25 000–30 000 km^2), about 40 RSET-MH instruments suffice to collect useful data. Rates of RSLR obtained from this approach are substantially higher than rates as inferred from tide-gauge data. We therefore conclude that LECZs may be at higher risk of flooding within a shorter time horizon than previously assumed.

1 Introduction

In the current era of accelerated sea-level rise, accurate measurements of relative sea-level change are critical to predict the conditions that coastal areas will face in the coming decades and beyond. Such measurements traditionally come from tide gauges, which provide the longest available instrumental records of relative sea-level rise (RSLR). Some of the oldest tide gauges have records spanning 150–200 or more years (e.g., Key West, USA, Maul and Martin, 1993; Brest, France; Świnoujście, Poland; New York, USA; and San Francisco, USA, Woodworth et al., 2011; and Boston, USA, Talke et al., 2018). Tide-gauge data have played a central role in calculations of global sea-level rise (e.g., Gornitz et al., 1982) and they continue to do so today (e.g., Church and White, 2011; Church et al., 2013; Hay et al., 2015).

Tide-gauge data are also heavily relied upon to evaluate the vulnerability of low-elevation coastal zones (LECZs) (e.g., Syvitski et al., 2009; Nicholls and Cazenave, 2010; Kopp et al., 2014; Pfeffer and Allemand, 2016). LECZs include large deltas and coastal plains that have often accumulated thick packages (tens of meters or more) of highly compressible Holocene strata and are home to some of the world's largest population centers (e.g., Tokyo, Shanghai, Bangkok, Manila) that are increasingly at risk due to RSLR. At the regional level, tide-gauge data have been used to study a variety of spatially variable processes. For example, in coastal Louisiana, the largest LECZ in the United States, tide-gauge data have been used to measure land subsidence (Swanson and Thurlow, 1973), the acceleration of RSLR (Nummedal, 1983), multi-decadal rates of subsidence and RSLR (Penland and Ramsey, 1990), and the impact of fluid extraction on RSLR (Kolker et al., 2011).

The Permanent Service for Mean Sea Level (PSMSL; http://www.psmsl.org, last access: 3 January 2019; Holgate et al., 2013) maintains records for nearly 2000 tide gauges globally, including 5 in coastal Louisiana: Eugene Island (data from 1939–1974), Grand Isle (1947–present), South Pass (1980–1999), Shell Beach (2008–present), and New Canal Station (2006–present). In many parts of the world, however, tide gauges with long, continuous records are few and far between. As a result, many studies of RSLR rely on tide-gauge records that are too short (longer than 50 years is preferable but at least 30 years is necessary to filter out natural variability due to phenomena such as storms, El Niño–Southern Oscillation cycles, changes in the orbital declination of the moon, shifts in ocean currents, and atmospheric pressure variability; Pugh, 1987; Douglas, 1991; Shennan and Woodworth, 1992), from inappropriate locations (e.g., outside of the area being studied), or both. For example, of the 32 tide gauges used by Syvitski et al. (2009), 21 were located outside the delta of interest, 11 had records of < 30 years, and 8 had both shortcomings. Furthermore, subsidence rates are highly spatially variable, often increasing or decreasing 2- to 4-fold within short distances (a few kilometers or less) as a result of subsurface fluid withdrawal and differential compaction, among other factors (e.g., Teatini et al., 2005; Törnqvist et al., 2008; Minderhoud et al., 2017; Koster et al., 2018; also see the review by Higgins, 2016). As a result, tide gauges provide limited information on subsidence rates beyond the instrument's immediate surroundings. Even if a tide gauge has a sufficiently long record and is appropriately located, it is critical to determine what processes the tide gauge is measuring and what it is not measuring. In LECZs, this is commonly not straightforward.

Tide gauges measure RSLR with respect to a nearby set of benchmarks. Leveling campaigns are conducted regularly (for example, at least once every 6 months for National Oceanic and Atmospheric Administration, NOAA, tide gauges; NOAA, 2013) to account for any changes in the elevation of the tide gauge with respect to these reference points. Tide gauges are typically leveled using a benchmark designated as the primary benchmark; secondary benchmarks are used to assess the stability of the primary benchmark (NOAA, 2013).

Figure 1 shows a schematic of tide gauges and associated benchmarks in three contrasting environments. Along rocky coastlines, benchmarks are typically anchored directly onto bedrock that is exposed at the surface (Fig. 1a). A tide gauge in such a setting therefore measures RSLR with respect to the land surface. In contrast, benchmarks in LECZs are typically anchored at depth. In thin LECZs, which are defined herein as those with unconsolidated sediment packages < 20 m thick, benchmark foundations typically penetrate the surficial layer of unconsolidated (usually Holocene) sediment and are anchored in the underlying consolidated (usually Pleistocene) strata (Fig. 1b). In thick LECZs, defined as possessing unconsolidated sediment packages that are > 20 m
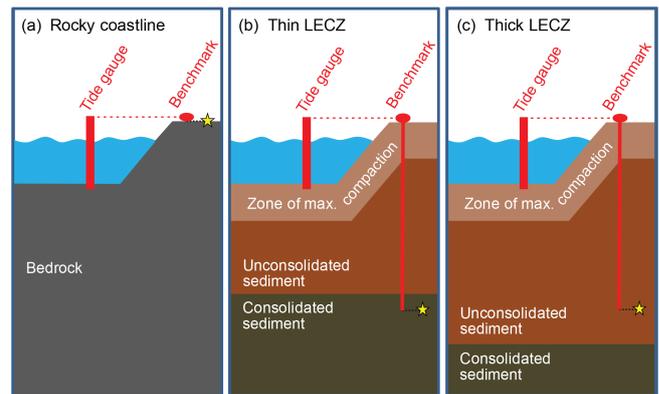

Figure 1. Schematic of a tide gauge and associated benchmark on a rocky coastline **(a)**, a thin LECZ **(b)**, and a thick LECZ **(c)**. In all three environments, the tide gauge measures RSLR with respect to the base of the benchmark foundation, which is indicated by a star in each panel.

thick, benchmark foundations are generally not sufficiently deep to reach the consolidated strata and are anchored within the unconsolidated sediment (Fig. 1c).

Regardless of the environment, all tide gauges measure changes in water surface elevation with respect to the foundation depth of their associated benchmarks. As a result, tide gauges with benchmarks anchored at depth do not account for processes occurring in the shallow subsurface above the benchmark foundation (Cahoon, 2015). For the purposes of this study, we define the subsidence that occurs above a benchmark's foundation as "shallow subsidence" (sensu Cahoon et al., 1995). Subsidence below a benchmark's foundation is termed "deep subsidence". In coastal Louisiana, at least 60 % of subsidence occurs in the shallowest 5–1 m (Jankowski et al., 2017). Tide gauges with benchmarks anchored at depth do not record this key component of RSLR (Cahoon, 2015). This issue was also recognized by Jankowski et al. (2017) and Nienhuis et al. (2017), but neither study elaborated on this problem. Here, we present a detailed assessment of benchmark information associated with tide gauges, followed by a discussion of its implications as well as methods to remedy this issue.

In order to better understand the contribution of vertical ground motion to RSLR, tide-gauge data are often used in conjunction with global navigation satellite system (GNSS) data (e.g., Mazzotti et al., 2009; Wöppelmann et al., 2009; Wöppelmann and Marcos, 2016; see also the Intergovernmental Oceanographic Commission manuals on sea-level measurement and interpretation, available at http://www.psmsl.org/train_and_info/training/manuals/, last access: 3 January 2019). In LECZs, GNSS stations are typically mounted on existing buildings or attached to rods that are driven to refusal (i.e., the depth at which friction prevents deeper penetration; see International GNSS Service station information at http://www.igs.org/network, last ac-

cess: 3 January 2019, and National Geodetic Survey station information at https://www.ngs.noaa.gov/CORS/, last access: 25 October 2018) and record the deep subsidence that occurs beneath their foundations. Similar to tide gauges, GNSS stations are nearly always anchored at depth and thus face many of the same concerns: they do not record shallow subsidence that occurs in the strata above the depth of their foundations.

Accurate measurements of RSLR are vital to predict the sustainability of world deltas and for communities in LECZs to adapt to their changing coastlines. In this study, we investigate the nature of tide-gauge benchmarks and GNSS station foundations in coastal Louisiana and assess the implications for measurements of RSLR and subsidence in LECZs worldwide. Reanalysis of time series from tide gauges and GNSS stations is not the purpose of our study. Instead, we present an alternative approach to measuring RSLR in LECZs through which shallow subsidence is determined using the rod surface-elevation table–marker horizon method (RSET-MH; see Webb et al., 2013, and Cahoon, 2015, for detailed descriptions of this method) and deep subsidence is determined using GNSS data. Using the Mississippi Delta (a thick LECZ) and the Chenier Plain (a thin LECZ) in coastal Louisiana as the primary study areas, we determine benchmark foundation depths and the type of strata in which the foundations are anchored. This allows us to determine which subsidence processes are measured by tide gauges and GNSS stations and to evaluate their usefulness as recorders of RSLR. We then place our findings in the context of LECZs worldwide. Our results suggest that tide gauges (and existing analyses of tide-gauge data) in these environments may underestimate rates of RSLR as observed at the land surface, and as a result, many LECZs may be at higher risk of submergence than previously recognized.

2 Data and methods

Relative sea-level and subsidence data are abundant in the Mississippi Delta and Chenier Plain, making coastal Louisiana an excellent target to assess methods of measuring RSLR. Records for at least 131 operational or previously operational tide gauges in this region are maintained by NOAA (https://tidesandcurrents.noaa.gov, last access: 3 January 2019), the US Army Corps of Engineers (USACE; http://www.rivergages.com, last access: 25 October 2018, and Veatch, 2017), and the US Geological Survey (USGS; http://nwis.waterdata.usgs.gov, last access: 3 January 2019). Although 37 of these tide gauges have records spanning more than 30 years, many of their records are incomplete and have large data gaps. Many other tide gauges in coastal Louisiana have short records; nearly half have time series < 10 years and a quarter are < 2 years long (see Table S1 in the Supplement for information on all 131 tide gauges).

By means of exhaustive record combing of NOAA, US-ACE, and USGS archives, benchmark foundation depths were determined for tide gauges located in the Holocene landscape of the Mississippi Delta and Chenier Plain. Foundation depths were then compared to the local elevation of the Pleistocene surface (with respect to the North American Vertical Datum of 1988, NAVD 88; Heinrich et al., 2015). Because the land surface elevations at the tide-gauge locations are close to sea level, the elevation of the Pleistocene surface is essentially equivalent to its depth beneath the land surface. When a tide gauge is associated with multiple benchmarks, the benchmark with the deepest known foundation was used for this analysis. For comparison, the analysis was repeated using primary benchmarks only.

A similar approach was taken to determine the foundation depths of GNSS stations. GNSS station information was compiled from Dokka et al. (2006) and Karegar et al. (2015). Of the 45 GNSS stations used for analysis by one or both studies, 17 are located in the Holocene landscape of coastal Louisiana. GNSS station foundation depths were compared to the local depth of the Pleistocene surface, similar to what was done for the tide gauges.

3 Results

The 131 tide gauges in coastal Louisiana were examined for benchmark information (Table S1, Fig. 2). Benchmark foundation depths are available for only 35 tide gauges (Table 1), including 31 maintained by NOAA and 4 maintained by USACE (see Table S1 for information on all 131 tide gauges). Each of these NOAA tide gauges is associated with 3 to 11 benchmarks (mean = 6 benchmarks), 77 % of which have known foundation depths. The total number of associated benchmarks is unknown for the USACE tide gauges. Benchmarks with known foundation depths are typically mounted on steel rods driven to refusal. Benchmarks with unknown foundation depths are typically mounted on concrete structures of a variety of types (e.g., building foundations, bridge abutments, and seawalls). These concrete structures are likely to have foundations that extend into the subsurface, but specific construction details are unknown. It is important to note that an unknown foundation depth should not be interpreted as a foundation depth of zero. The remaining 96 tide gauges (73 % of the total) have no available benchmark foundation information.

For tide gauges with available benchmark information, benchmark foundation depths range from 0.9 to 35.1 m, with a mean of 21.0 ± 5.4 m and a median of 20.7 m. The deepest known benchmarks are anchored an average of 21.5 ± 7.4 m below the ground surface, with a median depth of 23.2 m. Comparing this mean to the mean foundation depth of primary benchmarks (21.4 ± 3.9 m, $n = 23$), we find that there is no meaningful difference. Note that for 8 of these 23 tide gauges (35 %), the primary benchmark is also the benchmark
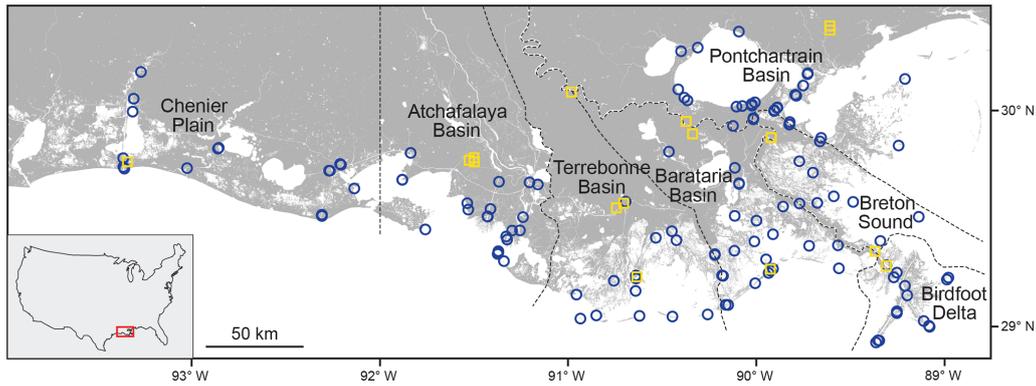
Figure 2. Location of tide gauges (circles, $n = 131$) and GNSS stations (squares, $n = 17$) in the Holocene landscape of coastal Louisiana. Dashed lines delineate geographic areas discussed in the text.
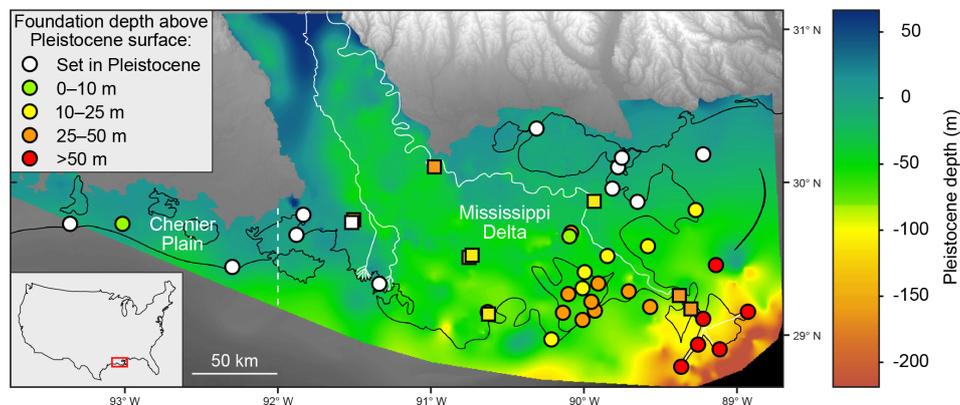

Figure 3. Elevation of the Pleistocene surface in coastal Louisiana (with respect to NAVD 88), which approximates the depth of the Pleistocene surface beneath the land surface given land surface elevations close to mean sea level. Circles and squares indicate tide gauge and GNSS station locations, respectively, and are color coded according to foundation height above the Pleistocene surface. Note that two GNSS stations (ENG1 and ENG2; see Table 2) have the same coordinates (and the same foundation depth) and plot on top of one another. The dashed white line, located at longitude 92° W, divides the Mississippi Delta from the Chenier Plain. Solid white lines show the Mississippi and Atchafalaya rivers. Black lines indicate shorelines. Pleistocene depth information is from Heinrich et al. (2015).

with the deepest known foundation. The mean foundation depth for the shallowest known benchmarks is 17.3 ± 7.0 m.

Figure 3 shows the location of tide gauges in coastal Louisiana (circles) and the foundation depth of their associated benchmarks relative to the local depth to the Pleistocene surface. The depth to the Pleistocene surface from the land surface at tide-gauge locations ranges from 5 to 142 m, with a mean of 47 ± 34 m and a median of 44 m (Fig. 4). Thus, benchmark foundations are anchored an average of 26 m above the Pleistocene surface. Only 11 of the 35 tide gauges (31 %) have benchmarks anchored in Pleistocene strata; the remaining 24 tide gauges (69 %) have benchmarks anchored in Holocene strata.

Of the 17 GNSS stations in coastal Louisiana, 10 (59 %) have known foundation depths (Table 2, Fig. 3). Information for all 17 GNSS stations in coastal Louisiana is available in Table S2. Foundation depths of the 10 GNSS stations range from 1 to 36.5 m, with a mean of $> 14.3 \pm 11.9$ m and a me-

dian of 14.9 m (Table 2). Note that for two GNSS stations only minimum foundation depths are available; these minimum values are used in the analysis in order to produce conservative results. At GNSS station locations, the depth to the Pleistocene surface ranges from 10 to 78 m, with a mean of 39 ± 20 m and a median of 35 m (Fig. 4). Thus, GNSS station foundations are anchored an average of 25 m above the Pleistocene surface. Only 1 of the 10 GNSS stations (10 %) is anchored in Pleistocene strata, whereas the remaining 9 GNSS stations (90 %) are anchored in Holocene strata. Figure 3 shows the location of GNSS stations in coastal Louisiana (squares) and their foundation depth relative to the local depth to the Pleistocene surface.

Table 1. Tide gauges in the Holocene landscape of coastal Louisiana with known foundation information ($n = 35$).

Tide-gauge name	Agency	Latitude	Longitude	Maximum benchmark foundation depth (m)	Depth to Pleistocene surface (m)	Benchmark foundation height above Pleistocene surface (m)
Amerada Pass	NOAA	29.4500	−91.3383	27.4	21	Set in Pleistocene
Barataria Waterway	USACE	29.6694	−90.1106	7.4	36	29
Bay Gardene	NOAA	29.5983	−89.6183	23.2	43	20
Bay Rambo	NOAA	29.3617	−90.1400	24.4	54	30
Bayou Petit Caillou	USACE	29.2543	−90.6635	24.4	57	33
Bayou St. Denis	NOAA	29.4967	−90.0250	23.2	44	21
Billet Bay	NOAA	29.3717	−89.7517	21.9	52	30
Breton Island	NOAA	29.4933	−89.1733	16.8	70	53
Calcasieu Pass	NOAA	29.7683	−93.3433	25	18	Set in Pleistocene
Caminada Pass	NOAA	29.2100	−90.0400	21.9	55	33
Chef Menteur Pass	NOAA	30.0650	−89.8000	35.1	13	Set in Pleistocene
Comfort Island	NOAA	29.8233	−89.2700	16.8	38	21
Cypremort Point	NOAA	29.7133	−91.8800	19.4	10	Set in Pleistocene
East Bay	NOAA	29.0533	−89.3050	14.6	106	91
East Timbalier Island	NOAA	29.0767	−90.2850	28.8	46	17
Freshwater Canal Locks	NOAA	29.5517	−92.3050	17.1	15	Set in Pleistocene
Grand Isle	NOAA	29.2633	−89.9567	19.8	57	37
Grand Pass	NOAA	30.1267	−89.2217	23.2	15	Set in Pleistocene
Greens Ditch	NOAA	30.1117	−89.7600	21.9	8	Set in Pleistocene
Hackberry Bay	NOAA	29.4017	−90.0383	30.5	52	22
Lafitte	NOAA	29.6667	−90.1117	30.5	37	7
Lake Judge Perez	NOAA	29.5583	−89.8833	24.4	39	15
Leeville	NOAA	29.2483	−90.2117	28	57	29
Martello Castle	NOAA	29.9450	−89.8350	19.51	19	Set in Pleistocene
Mendicant Island	NOAA	29.3183	−89.9800	24.4	55	31
Mermentau River	USACE	29.7704	−93.0135	1.5	6	5
North Pass	NOAA	29.2050	−89.0367	15.2	142	127
Pass Manchac	NOAA	30.2967	−90.3117	20.7	15	Set in Pleistocene
Pelican Island	NOAA	29.2667	−89.5983	21.9	64	42
Pilottown	NOAA	29.1783	−89.2583	32	88	56
Port Eads	USACE	29.0147	−89.1658	0.9	128	127
Shell Beach	NOAA	29.8683	−89.6733	27.4	27	Set in Pleistocene
Southwest Pass	NOAA	28.9250	−89.4183	24.4	109	85
St. Mary's Point	NOAA	29.4317	−89.9383	24.4	50	26
Weeks Bay	NOAA	29.8367	−91.8367	14.3	5	Set in Pleistocene

4 Discussion

4.1 Implications for the interpretation of tide-gauge and GNSS records

In coastal Louisiana, foundation information for tide-gauge benchmarks and GNSS stations is often not available, essentially precluding the interpretation of resulting time series in terms of rates of RSLR. Although many of the tide gauges listed in Table 1 are not useful for RSLR analyses due to their short records, all of the benchmarks used for the present analysis are currently published and considered stable. Furthermore, some of the tide gauges that currently have

short time series could become important in the future as their records become longer (e.g., Shell Beach). Because all tide-gauge benchmarks with known foundation information are anchored at depth rather than at ground level, and most (91 %) are anchored well below the land surface (> 10 m), their interpretation is far from straightforward. Tide gauges with benchmarks anchored at depth measure deep subsidence plus the component of RSLR associated with changes in real (geocentric) ocean level, but do not capture shallow subsidence, often a dominant element of total subsidence in this region. Similarly, all GNSS stations are anchored at depth (60 % are anchored > 10 m deep) and also do not record shallow subsidence. Thus, tide gauges and GNSS stations in

Table 2. GNSS stations in the Holocene landscape of coastal Louisiana with known foundation information ($n = 10$).

GNSS station code	Latitude	Longitude	Foundation depth (m)	Depth to Pleistocene surface (m)	Foundation height above Pleistocene surface (m)	Data source
AWES	30.10	−90.98	1	29	28	Karegar et al. (2015)
BVHS	29.34	−89.41	> 20	62	< 42	Dokka et al. (2006); Karegar et al. (2015)
ENG1	29.88	−89.94	~ 3	27	~ 24	Karegar et al. (2015)
ENG2	29.88	−89.94	~ 3	27	~ 24	Dokka et al. (2006)
FRAN	29.80	−91.53	14.7	10	Set in Pleistocene	Dokka et al. (2006)
FSHS	29.81	−91.50	1	15	14	Karegar et al. (2015)
HOMA	29.57	−90.76	18.3	40	22	Dokka et al. (2006)
HOUM	29.59	−90.72	> 15	40	< 25	Dokka et al. (2006); Karegar et al. (2015)
LMCN	29.25	−90.66	36.5	57	21	Dokka et al. (2006); Karegar et al. (2015)
VENI	29.28	−89.36	30.5	78	48	Dokka et al. (2006)

coastal Louisiana systematically underestimate the rates of local RSLR and subsidence, respectively.

Many tide gauges in coastal Louisiana have benchmarks that are mounted on existing concrete structures. The primary benchmark for the Grand Isle tide gauge, for example, is mounted on a seawall. Similar to tide gauges that measure RSLR with respect to a benchmark mounted on a steel rod driven to depth, the Grand Isle tide gauge produces a time series of RSLR with respect to the foundation of the concrete structure into which its primary benchmark is mounted. Although we were unable to acquire construction details for the seawall at Grand Isle, it is highly unlikely that it is simply resting on the land surface. We expect that the seawall foundation extends at least several meters into the subsurface in order to provide stability and protection for the adjacent Grand Isle Coast Guard station. Five other tide gauges also have primary benchmarks anchored on concrete structures: Caminada Pass, East Bay, Freshwater Canal Locks, Lafitte, and Martello Castle. Although all of these primary benchmarks are likely anchored at some depth below the surface, it is conceivable that their foundations are shallower than that of the deepest benchmarks (e.g., 19.8 m at Grand Isle). This may reduce the underestimation of the rate of RSLR measured by these tide gauges.

On the other hand, the RSET-MH data presented by Jankowski et al. (2017) suggest that shallow subsidence occurs dominantly in the uppermost 5 m in coastal Louisiana. Using data from 274 monitoring stations, Jankowski et al. (2017) calculated a mean shallow subsidence rate of 6.8 ± 7.9 mm year^{-1}. Limiting this analysis to stations where the instrument is anchored in Pleistocene strata and the overlying (Holocene) strata are < 5 m thick, we find a mean shallow subsidence rate of 6.4 ± 5.4 mm year^{-1} ($n = 55$). The similarity between these two numbers suggests that shallow subsidence is concentrated in the uppermost 5 m in this region. The implication would be that tide gauges with benchmarks anchored as little as 5 m below the surface would still not capture shallow subsidence and thus underestimate the rate of RSLR.

If a tide-gauge benchmark is anchored in Pleistocene deposits, deep subsidence consists solely of subsidence within the Pleistocene and underlying strata (Fig. 1b). This scenario is common in LECZs with a relatively thin Holocene sediment package, such as the Chenier Plain. In the Chenier Plain, the Pleistocene surface subsides at a rate of $\sim$ 1 mm year^{-1}, yet the wetland surface is subsiding notably faster at a rate of 7.5 mm year^{-1} on average (Jankowski et al., 2017). The remaining 6.5 mm year^{-1} of shallow subsidence occurs above the depth of local benchmark foundations and is typically not captured by tide gauges in this region.

In the case of a benchmark that is anchored in Holocene strata, deep subsidence also includes subsidence of the part of the Holocene sediment column that underlies the benchmark foundation. This scenario (Fig. 1c) is common in LECZs with thick sediment packages, such as the Mississippi Delta, and further complicates the interpretation of tide-gauge data. Compaction of deeper Holocene strata may result in an increase in the measured rate of RSLR when compared to tide gauges with benchmarks anchored in Pleistocene strata. However, tide gauges with benchmarks anchored in Holocene strata still record rates of RSLR that are considerably lower than what is seen at the land surface in the Mississippi Delta (13 ± 9 mm year^{-1}; Jankowski et al., 2017). For example, Kolker et al. (2011) and Karegar et al. (2015) calculated modern RSLR rates from tide-gauge data in the Mississippi Delta of $\sim$ 3 mm year^{-1} (after adding the long-term rate of RSLR measured at Pensacola, Florida) and at least $\sim$ 7 mm year^{-1}, respectively.
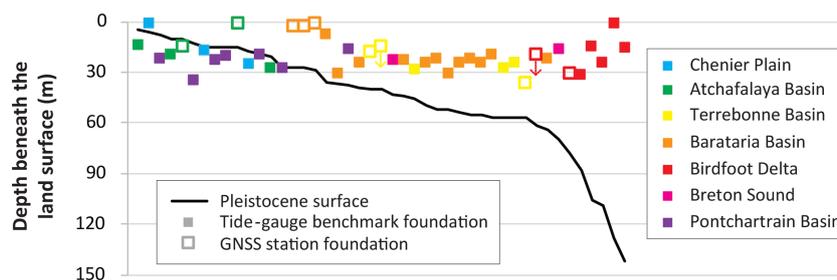
Figure 4. Schematic dip-oriented cross section comparing the depth of tide-gauge benchmarks and GNSS station foundations to the local depth to the Pleistocene surface. Sites are arranged by increasing depth of the Pleistocene surface. Note that two GNSS stations have minimum foundation depths (see Table 2), indicated here by small, downward-pointing arrows. See Fig. 2 for the location of geographic areas.

Table 3. Holocene sediment thicknesses of LECZs around the world, measured close to the shoreline where coastal strata tend to be the thickest.

Low-elevation coastal zone	Maximum thickness (m)	LECZ type	Reference
Chenier plain, Miranda, New Zealand	3–5	thin	Woodroffe et al. (1983)
Chenier Plain, SW Louisiana, USA	5–10	thin	Heinrich et al. (2015)
Venice Lagoon, Italy	10–15	thin	Zecchin et al. (2009)
Chao Phraya Delta, Thailand	10–15	thin	Tanabe et al. (2003a)
Vistula Delta, Poland	10–20	thin	Mojski (1995)
Rhine-Meuse Delta, the Netherlands	20–25	thick	Hijma et al. (2009)
Huanghe Delta (modern), China	20–25	thick	Xue (1993); Yi et al. (2003)
Po Delta, Italy	20–25	thick	Amorosi et al. (2017)
Tokyo Lowland, Japan	20–60	thick	Tanabe et al. (2015)
Mekong Delta, Vietnam	25–40	thick	Ta et al. (2002); Tanabe et al. (2003b)
Nobi Plain, Japan	30–40	thick	Hori et al. (2011)
Shatt al-Arab Delta, Iraq	30–40	thick	Larsen (1975)
Nile Delta, Egypt	30–50	thick	Stanley and Warne (1993)
Song Hong Delta, Vietnam	35–40	thick	Funabiki et al. (2007)
Fly Delta, Papua New Guinea	35–45	thick	Harris et al. (1993)
Ganges–Brahmaputra Delta, Bangladesh	50–100	thick	Goodbred and Kuehl (2000)
Mississippi Delta, SE Louisiana, USA	50–100	thick	Heinrich et al. (2015)
Yangtze Delta, China	60–90	thick	Li et al. (2000)
Indus Delta, Pakistan	110–120	thick	Clift et al. (2010)

Around the world, many LECZs have sediment packages that exceed 20 m in thickness, and some are as thick as 100 m or more (Table 3). Benchmarks in these areas are likely constructed in a broadly similar fashion to those in coastal Louisiana: either attached to rods driven to refusal or mounted on existing structures with non-negligible foundation depths. Tide-gauge benchmarks in the Netherlands, for example, are anchored 5–25 m deep (Rena Hoogland, personal communication, 2018) and generally reach the Pleistocene basement except in areas where the Holocene sediment thickness is greatest (Table 4). Thus, conditions in the Netherlands are roughly comparable to those in the Chenier Plain of coastal Louisiana (and likely other "thin" LECZs): tide gauges do not capture the shallow subsidence component of RSLR, but because benchmarks are generally anchored in a relatively stable substrate they are easier to interpret than many of the tide gauges in the Mississippi Delta (and likely other "thick" LECZs) where benchmarks are essentially "floating" in the Holocene succession.

In LECZs globally, tide gauges likely underestimate the local rate of RSLR. A lack of reliable RSLR data will be increasingly problematic in several large deltas that are home to major population centers (e.g., Ganges–Brahmaputra, Song Hong, Yangtze, Mekong, Nile) and are experiencing rapid subsidence (Alam, 1996; Mathers and Zalasiewicz, 1999; Shi et al., 2008; Erban et al., 2014; Gebremichael et al., 2018). In these areas and in LECZs globally, people and infrastructure may therefore be even more vulnerable to flooding than previously recognized (e.g., Syvitski et al., 2009; Tessler et al., 2015).

Two studies that considered delta vulnerability on a global scale (Ericson et al., 2006; Tessler et al., 2015) are notewor-

Table 4. Benchmark foundation depths and local depth to the Pleistocene surface for tide gauges in the Netherlands. Benchmark depths from Rena Hoogland, personal communication, 2018. Pleistocene surface depths are from Vos et al. (2011).

Tide-gauge name	Agency	Latitude	Longitude	Benchmark foundation depth (m)	Depth to Pleistocene surface (m)	Benchmark foundation height above Pleistocene surface (m)
Vlissingen	Rijkswaterstaat	51.4422	3.5961	17.6	4–6	Set in Pleistocene
Hoek van Holland	Rijkswaterstaat	51.9775	4.1200	14	20–22	6–8
IJmuiden	Rijkswaterstaat	52.4622	4.5547	13	18–20	5–7
Den Helder	Rijkswaterstaat	52.9644	4.7450	5–25	2–4	Set in Pleistocene
Harlingen	Rijkswaterstaat	53.1756	5.4094	5–25	4–6	Likely set in Pleistocene
Delfzijl	Rijkswaterstaat	53.3264	6.9331	20	6–8	Set in Pleistocene

thy because they did not depend on tide-gauge data. These studies determined RSLR by adding the historic rate of real (geocentric) sea-level rise to natural and anthropogenic subsidence data (Ericson et al., 2006) or by combining sea-level rise from satellite altimetry with subsidence estimates associated with fluid extraction (Tessler et al., 2015). While these approaches bypass the problems with tide gauges discussed above, they are also inherently limited by the need to characterize individual deltas by single metrics, by relying on measurements of global rather than local sea-level rise, and/or by not considering all major subsidence processes (notably shallow compaction). In the next section, we build on the recent study by Jankowski et al. (2017) to offer an alternative approach to measure RSLR in LECZs.

4.2 An alternative method for measuring present-day rates of relative sea-level rise

In order to accurately measure present-day RSLR in LECZs, we propose an alternative approach that combines measurements of shallow subsidence from RSET-MHs with measurements of deep subsidence and the oceanic component of sea-level rise from GNSS and satellite altimetry data, respectively (Fig. 5). This approach results in RSLR measurements expressed with respect to the land surface and eliminates the need for tide-gauge data. Nevertheless, we stress that best scientific practices will make use of all available data and compare the results of various measurement techniques. Furthermore, tide gauges remain critical for measuring many other processes, including tides (the original purpose of tide gauges) and event-scale phenomena such as storm surge, and remain invaluable in this regard.

In principle, both GNSS stations and tide gauges could be used to measure deep subsidence and these data could then be combined with measurements of shallow subsidence (plus geocentric sea-level rise in the case of GNSS data) to calculate RSLR. However, tide gauges must have sufficiently long time series (at least 30 years) and known foundation depths to be useful in this context. In coastal Louisiana, the number of tide gauges that meet these criteria ($n = 5$) are fewer
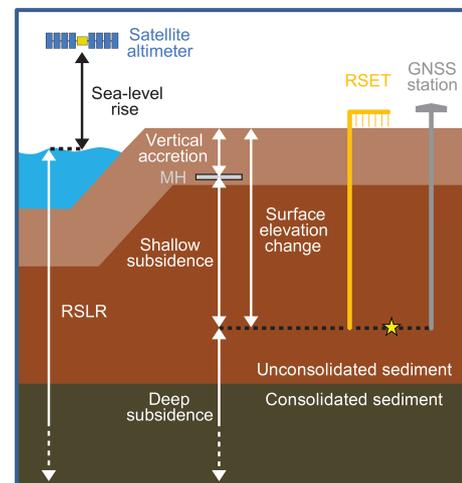

Figure 5. Schematic of combined instrumentation that includes an RSET-MH, which measures shallow subsidence, and a GNSS station, which measures deep subsidence. To measure shallow subsidence using an RSET-MH, surface elevation change is subtracted from vertical accretion (Cahoon, 2015). Surface elevation change is the change in height from a horizontal arm at a fixed elevation to the wetland surface measured using vertical pins. Vertical accretion is the thickness of sediment that accumulates above a feldspar marker horizon. If constructed with similar foundation depths (as shown by the star), the RSET-MH and GNSS station collect data that are complementary and can be added together and combined with satellite altimetry data to calculate the rate of RSLR.

than the number of GNSS stations with known foundation depths ($n = 10$). Additionally, concerted efforts are currently underway to address the complexities regarding GNSS monumentation. At a newly constructed subsidence superstation located in the lower Mississippi Delta, for example, three GNSS instruments are anchored at different depths in order to obtain a depth-integrated subsidence profile (Allison et al., 2016). Although this type of analysis is new, it can greatly improve our understanding of subsidence in LECZs in the future. Furthermore, GNSS data are less susceptible to short-term environmental conditions (i.e., wind speed and di-
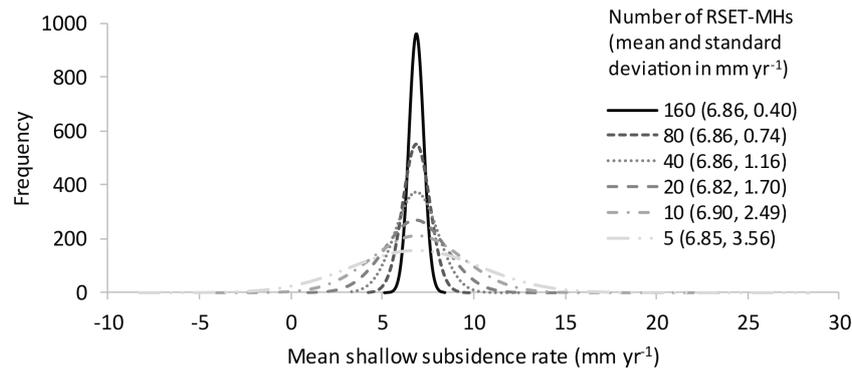
Figure 6. Probability density functions of the mean shallow subsidence rate for a given number of RSET-MHs calculated using a Monte Carlo simulation and 10 000 randomizations per analysis.

rection, tides, atmospheric pressure changes) than tide-gauge data. Thus, GNSS is the preferred method for measuring deep subsidence.

Although RSET-MHs, GNSS, and satellite altimetry all have unique limitations, technology is rapidly improving and reducing these shortcomings. Until recently, for example, satellite altimetry was ineffective in coastal areas (Cipollini et al., 2017). However, the launch of the Surface Water and Ocean Topography (SWOT; https://swot.jpl.nasa.gov/home.htm, last access: 3 January 2019) mission in 2021 is one of several efforts that are expected to significantly improve the quality of sea-surface records in the coastal zone and could therefore become an important element of the approach advocated here (Vignudelli et al., 2011). One remaining limitation of our proposed method of measuring RSLR is that RSET-MHs are only useful in wetland environments such as marshes (e.g., Day et al., 2011) and mangroves (e.g., Lovelock et al., 2015). However, space-based geodetic methods such as interferometric synthetic-aperture radar (InSAR) are effective at measuring subsidence rates (the sum of shallow and deep subsidence rates) in heavily human-modified delta environments (e.g., urban areas, agricultural land; Dixon et al., 2006; Jones et al., 2016; Da Lio et al., 2018) and can thus be complementary to RSET-MH datasets in this context. Care must be taken though to avoid reliance on permanent scatterers (e.g., buildings) with foundations at depth that may also not fully capture the shallow subsidence component. Ideally, RSET-MHs are installed with similar foundation depths as nearby GNSS stations in order to confirm that the two instruments are neither duplicating nor missing subsidence intervals. In coastal Louisiana, however, 33 % of GNSS stations have no known foundation information, and this lack of information is likely a common phenomenon worldwide.

Currently, coastal Louisiana has nearly 350 RSET-MHs operated by the USGS as part of the Coastwide Reference Monitoring System (CRMS; https://lacoast.gov/crms2, last access: 3 January 2019), which provide shallow subsidence data at high spatial resolution. Although data from a single

RSET-MH are commonly too noisy to produce a reliable trend (Jankowski et al., 2017), partly because most RSET-MHs were installed within the last decade and thus have time series that are mostly < 10 years long, such a high density of RSET-MHs is not necessary to produce adequate estimates of shallow subsidence rates for a wider region. Using a Monte Carlo approach, we took random samples from subsets of the full RSET-MH dataset for coastal Louisiana ($n = 274$) to determine the smallest sample size that would still produce reasonable outcomes with an acceptable error. While determining the acceptable error is inherently somewhat arbitrary, the results show that in coastal Louisiana a minimum of 40 RSET-MHs would be needed in order to produce a mean shallow subsidence rate with a sufficiently narrow 95 % confidence interval (4.54–9.18 mm year^{-1}; Fig. 6). In terms of density and given the size of coastal Louisiana (25 000–30 000 km^2), we estimate that two RSET-MHs per 1000 km^2 would suffice. Although this density is slightly higher than strictly needed in coastal Louisiana, it is conceivable that higher densities may be necessary in smaller LECZs.

In addition, averaging data from at least 40 RSET-MHs will encompass the high spatial variability commonly seen in shallow subsidence. In coastal Louisiana, spatial correlation in subsidence rates is largely limited to distances < 5 km, and no correlation exists beyond 25 km (Nienhuis et al., 2017). As a result, the relevance of a single measurement of shallow subsidence is limited to the area immediately around the instrument. Around the world, tide gauges are generally spaced tens if not hundreds of kilometers apart. Even if tide gauges had benchmarks anchored at the land surface and were able to measure shallow subsidence, there simply are not enough tide gauges with records that are sufficiently long for RSLR analysis to capture the large spatial variability in shallow subsidence. In LECZs worldwide, our ability to predict local rates of RSLR will improve as more RSET-MHs are added to a growing global network. We therefore echo Webb et al. (2013), who first proposed this type of global RSET-MH network, arguing that the instruments are low-cost and produce highly valuable measurements of shallow subsidence.

5   Conclusions

In the Mississippi Delta and Chenier Plain of coastal Louisiana, tide-gauge benchmarks and GNSS stations are anchored an average of 21.5 ± 7.4 m and $> 14.3 \pm 11.9$ m below the land surface, respectively. By comparison, the local depth to the Pleistocene surface averages 47 ± 34 m at tide-gauge locations and 39 ± 20 m at GNSS stations. Instruments located in the Chenier Plain, a thin LECZ with Holocene strata typically only 5–10 m thick, are generally anchored in consolidated Pleistocene strata. In the Mississippi Delta, an LECZ in which the Holocene sediment package is an order of magnitude thicker, tide-gauge benchmarks and GNSS stations are typically anchored within unconsolidated Holocene strata and therefore produce time series that are very difficult to interpret. Instruments anchored at depth do not capture shallow subsidence, a major component of total subsidence in this area. As a result, tide gauges and GNSS stations in coastal Louisiana, and likely in LECZs worldwide, underestimate rates of RSLR and subsidence with respect to the land surface by a variable but unknown amount.

In order to accurately measure present-day RSLR in LECZs, we propose an alternative method that combines measurements of shallow subsidence from RSET-MHs with measurements of deep subsidence and the oceanic component of sea-level rise from GNSS stations and satellite altimetry, respectively. This approach produces rates of RSLR that are explicitly tied to the land surface and eliminates the need for tide-gauge data in this context. We find that for an area the size of coastal Louisiana, a minimum density of two RSET-MHs per $1000\,\text{km}^2$ is necessary in order to obtain robust shallow subsidence data. We support the call for a global network of RSET-MHs as first put forward by Webb et al. (2013) and recently echoed by Osland et al. (2017). Data from such a global network will help refine existing plans for coastal adaptation that presently may be inadequate to deal with potentially higher-than-anticipated rates of RSLR.

Data availability.   All tide-gauge and GNSS data used in this article are provided in Tables S1 and S2 of the Supplement.

Supplement.   The supplement related to this article is available online at: https://doi.org/10.5194/os-15-61-2019-supplement.

Author contributions.   MEK conducted the research as a part of her PhD dissertation supervised by TET. MEK wrote the paper with input from TET.

Competing interests.   The authors declare that they have no conflict of interest.

References

Alam, M.: Subsidence of the Ganges-Brahmaputra Delta of Bangladesh and associated drainage, sedimentation and salinity problems, in: Sea-Level Rise and Coastal Subsidence, edited by: Milliman, J. D. and Haq, B. U., Springer, Dordrecht, the Netherlands, 169–192, https://doi.org/10.1007/978-94-015-8719-8_9, 1996.

Allison, M., Yuill, B., Törnqvist, T., Amelung, F., Dixon, T. H., Erkens, G., Stuurman, R., Jones, C., Milne, G., Steckler, M., Syvitski, J., and Teatini, P.: Global risks and research priorities for coastal subsidence, Eos, 97, 19, 22–27, https://doi.org/10.1029/2016EO055013, 2016.

Amorosi, A., Bruno, L., Cleveland, D. M., Morelli, A., and Hong, W.: Paleosols and associated channel-belt sand bodies from a continuously subsiding late Quaternary system (Po Basin, Italy): New insights into continental sequence stratigraphy, Geol. Soc. Am. Bull., 129, 449–463, https://doi.org/10.1130/B31575.1, 2017.

Cahoon, D. R.: Estimating relative sea-level rise and submergence potential at a coastal wetland, Estuar. Coast., 38, 1077–1084, https://doi.org/10.1007/s12237-014-9872-8, 2015.

Cahoon, D. R., Reed, D. J., and Day Jr., J. W.: Estimating shallow subsidence in microtidal salt marshes of the southeastern United States: Kaye and Barghoorn revisited, Mar. Geol., 128, 1–9, https://doi.org/10.1016/0025-3227(95)00087-F, 1995.

Church, J. A. and White, N. J.: Sea-level rise from the late 19th to the early 21st century, Surv. Geophys., 32, 585–602, https://doi.org/10.1007/s10712-011-9119-1, 2011.

Church, J. A., Clark, P. U., Cazenave, A., Gregory, J. M., Jevrejeva, S., Levermann, A., Merrifield, M. A., Milne, G. A., Nerem, R. S., Nunn, P. D., Payne, A. J., Pfeffer, W. T., Stammer, D., and Unnikrishnan, A. S.: Sea Level Change, in: Climate Change 2013: The Physical Science Basis, Contribution of Working Group I to the Fifth Assessment Report of the Intergovernmental Panel on Climate Change, edited by: Stocker, T. F., Qin, D., Plattner, G.-K., Tignor, M., Allen, S. K., Boschung, J., Nauels, A., Xia, Y., Bex, V., and Midgley, P. M., Cambridge University Press, New York, NY, USA, 1137–1216, 2013.

Cipollini, P., Calafat, F. M., Jevrejeva, S., Melet, A., and Prandi, P.: Monitoring sea level in the coastal zone with satellite altimetry and tide gauges, Surv. Geophys., 38, 33–57, https://doi.org/10.1007/978-3-319-56490-6_3, 2017.

Clift, P. D., Giosan, L., Carter, A., Garzanti, E., Galy, V., Tabrez, A. R., Pringle, M., Campbell, I. H., France-Lanord, C., Blusztajn, J., Allen, C., Alizai, A., Lückge, A., Danish, M., and Rabbani, M. M.: Monsoon control over erosion patterns in the Western Himalaya: possible feed-back into the tectonic evolution, Geol. Soc. Spec. Publ., 342, 185–218, https://doi.org/10.1144/SP342.12, 2010.

Da Lio, C., Teatini, P., Strozzi, T., and Tosi, L.: Understanding land subsidence in salt marshes of the Venice Lagoon from SAR interferometry and ground-based investigations, Remote Sens. Environ., 205, 56–70, https://doi.org/10.1016/j.rse.2017.11.016, 2018.

Day, J., Ibáñez, C., Scarton, F., Pont, D., Hensel, P., Day, J., and Lane, R.: Sustainability of Mediterranean deltaic and lagoon wetlands with sea-level rise: The importance of river input, Estuar. Coast., 34, 483–493, https://doi.org/10.1007/s12237-011-9390-x, 2011.

Dixon, T. H., Amelung, F., Ferretti, A., Novali, F., Rocca, F., Dokka, R., Sella, G., Kim, S.-W., Wdowinski, S., and Whitman, D.: Subsidence and flooding in New Orleans, Nature, 441, 587–588, https://doi.org/10.1038/441587a, 2006.

Dokka, R. K., Sella, G. F., and Dixon, T. H.: Tectonic control of subsidence and southward displacement of southeast Louisiana with respect to stable North America, Geophys. Res. Lett., 33, L23308, https://doi.org/10.1029/2006GL027250, 2006.

Douglas, B. C.: Global sea level rise, J. Geophys. Res., 96, 6981–6992, https://doi.org/10.1029/91JC00064, 1991.

Erban, L. E., Gorelick, S. M., and Zebker, H. A.: Groundwater extraction, land subsidence, and sea-level rise in the Mekong Delta, Vietnam, Environ. Res. Lett., 9, 084010, https://doi.org/10.1088/1748-9326/9/8/084010, 2014.

Ericson, J. P., Vörösmarty, C. J., Dingman, S. L., Ward, L. G., and Meybeck, M.: Effective sea-level rise and deltas: Causes of change and human dimension implications, Global Planet. Change, 50, 63–82, https://doi.org/10.1016/j.gloplacha.2005.07.004, 2006.

Funabiki, A., Haruyama, S., Van Quy, N., Van Hai, P., and Thai, D. H.: Holocene delta plain development in the Song Hong (Red River) delta, Vietnam, J. Asian Earth Sci., 30, 518–529, https://doi.org/10.1016/j.jseaes.2006.11.013, 2007.

Gebremichael, E., Sultan, M., Becker, R., El Bastawesy, M., Cherif, O., and Emil, M.: Assessing land deformation and sea encroachment in the Nile Delta: A radar interferometric and inundation modeling approach, J. Geophys. Res.-Sol. Ea., 123, 3208–3224, https://doi.org/10.1002/2017JB015084, 2018.

Goodbred, S. L. and Kuehl, S. A.: The significance of large sediment supply, active tectonism, and eustasy on margin sequence development: Late Quaternary stratigraphy and evolution of the Ganges–Brahmaputra delta, Sediment. Geol., 133, 227–248, https://doi.org/10.1016/S0037-0738(00)00041-5, 2000.

Gornitz, V., Lebedeff, S., and Hansen, J.: Global sea level trend in the past century, Science, 215, 1611–1614, https://doi.org/10.1126/science.215.4540.1611, 1982.

Harris, P. T., Baker, E. K., Cole, A. R., and Short, S. A.: A preliminary study of sedimentation in the tidally dominated Fly River Delta, Gulf of Papua, Cont. Shelf Res., 13, 441–472, https://doi.org/10.1016/0278-4343(93)90060-B, 1993.

Hay, C. C., Morrow, E., Kopp, R. E., and Mitrovica, J. X.: Probabilistic reanalysis of twentieth-century sea-level rise, Nature, 517, 481–484, https://doi.org/10.1038/nature14093, 2015.

Heinrich, P., Paulsell, R., Milner, R., Snead, J., and Peele, H.: Investigation and GIS development of the buried Holocene-Pleistocene surface in the Louisiana coastal plain, Louisiana Geological Survey and Louisiana State University for the Coastal Protection and Restoration Authority of Louisiana, Baton Rouge, LA, USA, 140 pp., 2015.

Higgins, S. A.: Advances in delta-subsidence research using satellite methods, Hydrogeol. J., 24, 587–600, https://doi.org/10.1007/s10040-015-1330-6, 2016.

Hijma, M. P., Cohen, K. M., Hoffmann, G., Van der Spek, A. J. F., and Stouthamer, E.: From river valley to estuary: The evolution of the Rhine mouth in the early to middle Holocene (western Netherlands, Rhine-Meuse delta), Neth. J. Geosci., 88, 13–53, https://doi.org/10.1017/S0016774600000986, 2009.

Holgate, S. J., Matthews, A., Woodworth, P. L., Rickards, L. J., Tamisiea, M. E., Bradshaw, E., Foden, P. R., Gordon, K. M., Jevrejeva, S., and Pugh, J.: New data systems and products at the Permanent Service for Mean Sea Level, J. Coastal Res., 29, 493–504, https://doi.org/10.2112/JCOASTRES-D-12-00175.1, 2013.

Hori, K., Usami, S., and Ueda, H.: Sediment facies and Holocene deposition rate of near-coastal fluvial systems: An example from the Nobi Plain, Japan, J. Asian Earth Sci., 41, 195–203, https://doi.org/10.1016/j.jseaes.2011.01.016, 2011.

Jankowski, K. L., Törnqvist, T. E., and Fernandes, A. M.: Vulnerability of Louisiana's coastal wetlands to present-day rates of relative sea-level rise, Nat. Commun., 8, 14792, https://doi.org/10.1038/ncomms14792, 2017.

Jones, C. E., An, K., Blom, R. G., Kent, J. D., Ivins, E. R., and Bekaert, D.: Anthropogenic and geologic influences on subsidence in the vicinity of New Orleans, Louisiana, J. Geophys. Res.-Sol. Ea., 121, 3867–3887, https://doi.org/10.1002/2015JB012636, 2016.

Karegar, M. A., Dixon, T. H., and Malservisi, R.: A three-dimensional surface velocity field for the Mississippi Delta: Implications for coastal restoration and flood potential, Geology, 43, 519–522, https://doi.org/10.1130/G36598.1, 2015.

Kolker, A. S., Allison, M. A., and Hameed, S.: An evaluation of subsidence rates and sea-level variability in the northern Gulf of Mexico, Geophys. Res. Lett., 38, L21404, https://doi.org/10.1029/2011GL049458, 2011.

Kopp, R. E., Horton, R. M., Little, C. M., Mitrovica, J. X., Oppenheimer, M., Rasmussen, D. J., Strauss, B. H., and Tebaldi, C.: Probabilistic 21st and 22nd century sea-level projections at a global network of tide-gauge sites, Earth's Future, 2, 383–406, https://doi.org/10.1002/2014EF000239, 2014.

Koster, K., Cohen, K. M., Stafleu, J., and Stouthamer, E.: Using ^{14}C-dated peat beds for reconstructing subsidence by compression in the Holland coastal plain of the Netherlands, J. Coastal Res., 34, 1035–1045, https://doi.org/10.2112/JCOASTRES-D-17-00093.1, 2018.

Larsen, C. E.: The Mesopotamian Delta region: A reconsideration of Lees and Falcon, J. Am. Oriental Soc., 95, 43–57, https://doi.org/10.2307/599157, 1975.

Li, C., Chen, Q., Zhang, J., Yang, S., and Fan, D.: Stratigraphy and paleoenvironmental changes in the Yangtze Delta dur-

ing the Late Quaternary, J. Asian Earth Sci., 18, 453–469, https://doi.org/10.1016/S1367-9120(99)00078-4, 2000.

Lovelock, C. E., Cahoon, D. R., Friess, D. A., Guntenspergen, G. R., Krauss, K. W., Reef, R., Rogers, K., Saunders, M. L., Sidik, F., Swales, A., Saintilan, N., Thuyen, L. X., and Triet, T.: The vulnerability of Indo-Pacific mangrove forests to sea-level rise, Nature, 526, 559–563, https://doi.org/10.1038/nature15538, 2015.

Mathers, S. and Zalasiewicz, J.: Holocene sedimentary architecture of the Red River Delta, J. Coastal Res., 15, 314–325, 1999.

Maul, G. A. and Martin, D. M.: Sea level rise at Key West, Florida, 1846–1992: America's longest instrument record?, Geophys. Res. Lett., 20, 1955–1958, https://doi.org/10.1029/93GL02371, 1993.

Mazzotti, S., Lambert, A., Van der Kooij, M., and Mainville, A.: Impact of anthropogenic subsidence on relative sea-level rise in the Fraser River delta, Geology, 37, 771–774, https://doi.org/10.1130/G25640A.1, 2009.

Minderhoud, P. S. J., Erkens, G., Pham, V. H., Bui, V. T., Erban, L., Kooi, H., and Stouthamer, E.: Impacts of 25 years of groundwater extraction on subsidence in the Mekong delta, Vietnam, Environ. Res. Lett., 12, 064006, https://doi.org/10.1088/1748-9326/aa7146, 2017.

Mojski, J. E.: Geology and evolution of the Vistula Delta and Vistula Bar, J. Coastal Res., 11, 141–149, 1995.

Nicholls, R. J. and Cazenave, A.: Sea-level rise and its impact on coastal zones, Science, 328, 1517–1520, https://doi.org/10.1126/science.1185782, 2010.

Nienhuis, J. H., Törnqvist, T. E., Jankowski, K. L., Fernandes, A. M., and Keogh, M. E.: A new subsidence map for coastal Louisiana, GSA Today, 27, 9, 58–59, https://doi.org/10.1130/GSATG337GW.1, 2017.

NOAA (National Oceanic and Atmospheric Administration): CO-OPS specifications and deliverables for installation, operation, and removal of water level stations, Center for Operational Oceanographic Products and Services, Engineering Division, National Ocean Service, Silver Spring, MD, USA, 30 pp., 2013.

Nummedal, D.: Future sea level changes along the Louisiana coast, Shore and Beach, 51, 2, 10–15, 1983.

Osland, M. J., Griffith, K. T., Larriviere, J. C., Feher, L. C., Cahoon, D. R., Enwright, N. M., Oster, D. A., Tirpak, J. M., Woodrey, M. S., Collini, R. C., Baustian, J. J., Breithaupt, J. L., Cherry, J. A., Conrad, J. R., Cormier, N., Coronado-Molina, C. A., Donoghue, J. F., Graham, S. A., Harper, J. W., Hester, M. W., Howard, R. J., Krauss, K. W., Kroes, D. E., Lane, R. R., McKee1, K. L., Mendelssohn, I. A., Middleton, B. A., Moon, J. A., Piazza, S. C., Rankin, N. M., Sklar, F. H., Steyer, G. D., Swanson, K. M., Swarzenski, C. M., Vervaeke, W. C., Willis, J. M., and Van Wilson, K.: Assessing coastal wetland vulnerability to sea-level rise along the northern Gulf of Mexico coast: Gaps and opportunities for developing a coordinated regional sampling network, PLoS ONE, 12, e0183431, https://doi.org/10.1371/journal.pone.0183431, 2017.

Penland, S. and Ramsey, K. E.: Relative sea-level rise in Louisiana and the Gulf of Mexico: 1908–1988, J. Coastal Res., 6, 323–342, 1990.

Pfeffer, J. and Allemand, P.: The key role of vertical land motions in coastal sea level variations: A global synthesis of multisatellite altimetry, tide gauge data and GPS measurements, Earth Planet.

Sc. Lett., 439, 39–47, https://doi.org/10.1016/j.epsl.2016.01.027, 2016.

Pugh, D. T.: Tides, Surges, and Mean Sea-Level, John Wiley and Sons, New York, NY, USA, 472 pp., 1987.

Shennan, I. and Woodworth, P. L.: A comparison of late Holocene and twentieth-century sea-level trends from the UK and North Sea region, Geophys. J. Int., 109, 96–105, https://doi.org/10.1111/j.1365-246X.1992.tb00081.x, 1992.

Shi, X., Wu, J., Ye, S., Zhang, Y., Xue, Y., Wei, Z., Li, Q., and Yu, J.: Regional land subsidence simulation in Su-Xi-Chang area and Shanghai City, China, Eng. Geol., 100, 27–42, https://doi.org/10.1016/j.enggeo.2008.02.011, 2008.

Stanley, D. J. and Warne, A. G.: Nile Delta: Recent geological evolution and human impact, Science, 260, 628–634, https://doi.org/10.1126/science.260.5108.628, 1993.

Swanson, R. L. and Thurlow, C. I.: Recent subsidence rates along the Texas and Louisiana coasts as determined from tide measurements, J. Geophys. Res., 78, 2665–2671, https://doi.org/10.1029/JC078i015p02665, 1973.

Syvitski, J. P. M., Kettner, A. J., Overeem, I., Hutton, E. W. H., Hannon, M. T., Brakenridge, G. R., Day, J., Vörösmarty, C., Saito, Y., Giosan, L., and Nicholls, R. J.: Sinking deltas due to human activities, Nat. Geosci., 2, 681–686, https://doi.org/10.1038/ngeo629, 2009.

Ta, T. K. O., Nguyen, V. L., Tateishi, M., Kobayashi, I., Tanabe, S., and Saito, Y.: Holocene delta evolution and sediment discharge of the Mekong River, southern Vietnam, Quaternary Sci. Rev., 21, 1807–1819, https://doi.org/10.1016/S0277-3791(02)00007-0, 2002.

Talke, S. A., Kemp, A. C., and Woodruff, J.: Relative sea level, tides, and extreme water levels in Boston Harbor from 1825 to 2018, J. Geophys. Res.-Oceans, 123, 3895–3914, https://doi.org/10.1029/2017JC013645, 2018.

Tanabe, S., Saito, Y., Sato, Y., Suzuki, Y., Sinsakul, S., Tiyapairach, S., and Chaimanee, N.: Stratigraphy and Holocene evolution of the mud-dominated Chao Phraya delta, Thailand, Quaternary Sci. Rev., 22, 789–807, https://doi.org/10.1016/S0277-3791(02)00242-1, 2003a.

Tanabe, S., Ta, T. K. O., Nguyen, V. L., Tateishi, M., Kobayashi, I., and Saito, Y.: Delta evolution model inferred from the Holocene Mekong delta, southern Vietnam, SEPM (Society for Sediment. Geol.) Special Publication, 76, 175–188, 2003b.

Tanabe, S., Nakanishi, T., Ishihara, Y., and Nakashima, R.: Millennial-scale stratigraphy of a tide-dominated incised valley during the last 14 kyr: Spatial and quantitative reconstruction in the Tokyo Lowland, central Japan, Sedimentology, 62, 1837–1872, https://doi.org/10.1111/sed.12204, 2015.

Teatini, P., Tosi, L., Strozzi, T., Carbognin, L., Wegmüller, U., and Rizzetto, F.: Mapping regional land displacements in the Venice coastland by an integrated monitoring system, Remote Sens. Environ., 98, 403–413, https://doi.org/10.1016/j.rse.2005.08.002, 2005.

Tessler, Z. D., Vörösmarty, C. J., Grossberg, M., Gladkova, I., Aizenman, H., Syvitski, J. P. M., and Foufoula-Georgiou, E.: Profiling risk and sustainability in coastal deltas of the world, Science, 349, 638–643, https://doi.org/10.1126/science.aab3574, 2015.

Törnqvist, T. E., Wallace, D. J., Storms, J. E. A., Wallinga, J., Van Dam, R. L., Blaauw, M., Derksen, M. S., Klerks, C. J. W., Mei-

jneken, C., and Snijders, E. M. A.: Mississippi Delta subsidence primarily caused by compaction of Holocene strata, Nat. Geosci., 1, 173–176, https://doi.org/10.1038/ngeo129, 2008.

Veatch, W.: 2015 updated atlas of U.S. Army Corps of Engineers historic daily tide data in coastal Louisiana, U.S. Army Corps of Engineers, New Orleans District, New Orleans, LA, USA, Mississippi River Geomorphology and Potamology Program Report, 14, 40 pp. 2017.

Vignudelli, S., Kostianoy, A. G., Cipollini, P., and Benveniste, J. (Eds.): Coastal Altimetry, Springer, Berlin, Germany, 578 pp., https://doi.org/10.1007/978-3-642-12796-0, 2011.

Vos, P. C., Bazelmans, J., Weerts, H. J. T., and Van der Meulen, M. J. (Eds.): Atlas van Nederland in het Holoceen, Bert Bakker, Amsterdam, the Netherlands, 94 pp., 2011.

Webb, E. L., Friess, D. A., Krauss, K. W., Cahoon, D. R., Guntenspergen, G. R., and Phelps, J.: A global standard for monitoring coastal wetland vulnerability to accelerated sea-level rise, Nat. Clim. Change, 3, 458–465, https://doi.org/10.1038/nclimate1756, 2013.

Woodroffe, C. D., Curtis, R. J., and McLean, R. F.: Development of a chenier plain, Firth of Thames, New Zealand, Mar. Geol., 53, 1–22, https://doi.org/10.1016/0025-3227(83)90031-2, 1983.

Woodworth, P. L., Menéndez, M., and Gehrels, W. R.: Evidence for century-timescale acceleration in mean sea levels and for recent changes in extreme sea levels, Surv. Geophys., 32, 603–618, https://doi.org/10.1007/s10712-011-9112-8, 2011.

Wöppelmann, G., Letetrel, C., Santamaria, A., Bouin, M.-N., Collilieux, X., Altamimi, Z., Williams, S. D. P., and Martín Míguez, B.: Rates of sea-level change over the past century in a geocentric reference frame, Geophys. Res. Lett., 36, L12607, https://doi.org/10.1029/2009GL038720, 2009.

Wöppelmann, G. and Marcos, M.: Vertical land motion as a key to understanding sea level change and variability, Rev. Geophys., 54, 64–92, https://doi.org/10.1002/2015RG000502, 2016.

Xue, C.: Historical changes in the Yellow River delta, China, Mar. Geol., 113, 321–329, https://doi.org/10.1016/0025-3227(93)90025-Q, 1993.

Yi, S., Saito, Y., Oshima, H., Zhou, Y., and Wei, H.: Holocene environmental history inferred from pollen assemblages in the Huanghe (Yellow River) delta, China: climatic change and human impact, Quaternary Sci. Rev., 22, 609–628, https://doi.org/10.1016/S0277-3791(02)00086-0, 2003.

Zecchin, M., Brancolini, G., Tosi, L., Rizzetto, F., Caffau, M., and Baradello, L.: Anatomy of the Holocene succession of the southern Venice lagoon revealed by very high-resolution seismic data, Cont. Shelf Res., 29, 1343–1359, https://doi.org/10.1016/j.csr.2009.03.006, 2009.